

On the Impact of Transposition Errors in Diffusion-Based Channels

Werner Haselmayr, Neeraj Varshney, A. Taufiq Asyhari, Weisi Guo and Andreas Springer

Published PDF deposited in Coventry University's Repository

Original citation:

Haselmayr et al. "On the impact of transposition errors in diffusion-based channels." *IEEE Transactions on Communications* 67.1 (2019): 364-374.

<http://dx.doi.org/10.1109/TCOMM.2018.2869568>

ISSN: 0090-6778

Publisher: IEEE

Copyright © and Moral Rights are retained by the author(s) and/ or other copyright owners. A copy can be downloaded for personal non-commercial research or study, without prior permission or charge. This item cannot be reproduced or quoted extensively from without first obtaining permission in writing from the copyright holder(s). The content must not be changed in any way or sold commercially in any format or medium without the formal permission of the copyright holders.

On the Impact of Transposition Errors in Diffusion-Based Channels

Werner Haselmayr, *Member, IEEE*, Neeraj Varshney, *Student Member, IEEE*, A. Taufiq Asyhari, *Member, IEEE*, Andreas Springer, *Member, IEEE*, and Weisi Guo*, *Member, IEEE*

Abstract— In this work, we consider diffusion-based molecular communication with and without drift between two static nanomachines. We employ type-based information encoding releasing single molecules per information bit. At the receiver we consider an asynchronous detection algorithm which exploits the arrival order of the molecules. In such systems transposition errors fundamentally undermine reliability and capacity. Thus, in this work we study the impact of transpositions on the system performance. We present an analytical expression for the exact bit error probability (BEP) caused by transposition and we derive computationally tractable approximations of the BEP for diffusion-based channels with and without drift. Based on these results we analyze the BEP when background is not negligible and we derive the optimal bit interval minimizing the BEP. We confirm the theoretical results through numerical results. Moreover, we show the error and goodput performance for different parameters such as block size or noise generation rate.

Index Terms—Asynchronous detection, diffusion-based channels, Lévy distribution, molecular communication, inverse Gaussian distribution, transposition effect

I. INTRODUCTION

MOLECULAR communication (MC) broadly defines the transmission of information using biochemical molecules over multiple distance scales [1], [2]. Within multicellular organisms, MC within cells, between local cells, and across the body of the organism (e.g., hormones) is essential for coordinated cellular action-reaction. Between organisms, MC takes place over several kilometers distance in air and under water (e.g., pheromones), and is used to signal intent, assist navigation, and warn of impending dangers [3]. The aforementioned MC largely relies on messenger molecules to transverse channels using some form of normal or anomalous diffusion mechanism, potentially combining microscopic discrete random walk with macroscopic continuum fluid mechanics.

Due to the potential for ultra-high energy efficiency [4], device dimension scalability, and bio-compatibility, diffusion-based MC has gathered intense research interest. **Currently, the majority of research in diffusion-based MC can be split**

between¹: i) Fundamental understanding and modeling of molecular signaling (e.g., [5]–[7]); ii) Design, fabrication and testing of human-made molecular communication systems (e.g., [8]–[10]); iii) Applying the MC paradigm to nanomedicine applications (e.g., [11]–[13]).

A. Motivation and Related Work

In diffusion-based MC the information can be encoded in the molecular concentration level, the release time of the molecules, and the type of molecules [2]. Moreover, a combination of the aforementioned techniques is also possible. Most existing work in MC considers information encoding in the molecular concentration level (e.g., [14] and the references therein). The detection algorithms are based on the received concentration level, which is sampled at predetermined time instants. The detector can rely on the law of large numbers, whereby the arrival time of the peak does not vary significantly. For concentration-encoded MC intersymbol interference is the dominant error source and a vast amount of work has been devoted to this issue in the past (e.g., [15] and the references therein).

However, since it is envisioned that MC employs nanomachines with very limited capabilities, it is very likely that molecular signals are represented by a limited set of molecules or molecular clusters rather than on the emission of a large number of molecules [16]. Here, the detection algorithms for time- and type-based information encoding exploit the arrival time or the arrival order of the molecules, respectively. Due to the stochastic nature of diffusion-based channels, it may occur that a sequence of transmitted molecules arrive out of order at the receiver, i.e. molecules that are released earlier arrive late – yielding so-called transpositions² of bits or symbols [17]. Thus, for time- and type-based information encoding using individual molecules transposition errors are the dominant error source. The implementation of an optimal maximum likelihood detector is almost impractical, even for a short sequence of molecules, since all possible permutations must be taken into account [6], [18]. For time-based information encoding a sub-optimal detector is proposed in [18], which cannot be adopted for type-based information encoding. For type-based information encoding the channel capacity is derived in [19], assuming only transpositions between neighboring bits. In [20], [21] the impact

¹Although most research activities fall in one of these categories, we are aware that there exists other areas where significant effort have been made.

²In [17], transpositions are referred to as crossovers.

Manuscript received month day, 2017; revised month day, year; accepted month day, year. *Corresponding author. W. Haselmayr and A. Springer are with the Johannes Kepler University Linz, Austria (email: {werner.haselmayr, andreas.springer}@jku.at). N. Varshney is with the Department of Electrical Engineering, Indian Institute of Technology Kanpur, India (email: neerajv@iitk.ac.in). A. T. Asyhari is with the Centre for Electronic Warfare, Information and Cyber, Cranfield University, United Kingdom (email: taufiq-a@ieee.org). W. Guo is with the School of Engineering, University of Warwick, United Kingdom (email: weisi.guo@warwick.ac.uk).

of transposition errors for diffusion-based MC with mobile transmit and receive nano-machines is investigated. Different techniques for mitigating transposition errors are considered in [16], [22]–[26]. These approaches can be divided into three categories: Sender-oriented, environment-oriented, and receiver-oriented. The works in [16], [22], [24]–[26] consider sender-oriented techniques. In [22] the bit interval is increased and in [16] multiple molecules per information bit are released, instead of a single molecule. Various block coding techniques are proposed in [24]–[26]. The code design is no longer based on the Hamming distance, which is only useful if the bits are corrupted by noise and is likely to be ineffective in the case of transposition errors. Thus, other attributes, such as for example the Hamming weight [26] or a molecular coding distance [24] are considered as suitable coding design paradigms. Environment-oriented approaches are presented in [22], [23]. In [22] different propagation mechanisms are investigated (diffusion, diffusion with amplification, diffusion in fixed volume space, motor-driven diffusion) and in [23] a Dielectrophoresis-based relay system is proposed to maintain in-sequence delivery of molecules. Such a system converts the random diffusion into a controlled and guided drift by collecting molecules on electrodes and relaying them at a controlled interval. In [22] a receiver-oriented approach is considered by introducing buffering at the receiver to recover the correct order.

Although the works in [16], [19], [22]–[26] consider different aspects of the transposition effect a comprehensive performance analysis, especially for diffusion-based channels without drift, is lacking in the current literature.

B. Contributions

In this work, we investigate the impact of transpositions on the performance of diffusion-based MC systems with and without drift. We employ type-based information encoding releasing single molecules per information bit and the asynchronous detection algorithm exploits the arrival order of the molecules. We present an analytical expression for the exact bit error probability (BEP), which takes all possible permutations into account. Since evaluating the exact BEP expression is only feasible for short sequences, we derive computationally tractable approximations of the BEP. For pure diffusion channels, we derive a tight upper bound based on the probability of out of order sequence delivery and the average BEP over these permutations. For drift channels, we approximate the BEP based on the observation that transpositions between neighboring bits are dominant. To the best of our knowledge, neither an exact BEP nor a tight bound for pure diffusion channels has been reported in related works [16], [19], [22]–[26] and the current literature. For drift channels, we obtain the same results as in [16], but we applied an alternative derivation, revealing some new insights. Additionally, we provide a theoretical BEP analysis when background noise is not negligible and derive the optimal bit interval minimizing the BEP. Through numerical results we show the error and goodput performance with and without background noise for different parameters and we confirm the theoretical results. It is important to

note that the presented study is important for all applications which require in-sequence delivery of single molecules, e.g., diagnostic (in-vitro) [27] and drug assessment systems [28].

C. Organization

The rest of the paper is organized as follows: Section II presents the system model and the considered propagation environment. In Section III we first derive the exact and approximate BEP caused by transpositions and then we investigate the BEP when background noise is not negligible. In Section IV we show the error and goodput performance with and without background noise through numerical results. Finally, Section V provides concluding remarks.

II. SYSTEM MODEL

We consider a semi-infinite one-dimensional (1D) fluid environment, whereby the length of propagation is large compared to width dimensions (e.g., blood vessels). We assume constant temperature T_a and viscosity η . A point transmitter (TX) and a point receiver (RX) are placed at a distance d . We consider the transmission of K information bits $\mathbf{b} = [b_1, \dots, b_K]$, where $b_k \in \{0, 1\}$ denotes the transmitted bit in the k th bit interval. We employ binary molecule shift keying [2], which maps bit 0 or bit 1 to a single molecule of type- a or type- b , respectively. Both molecule types have the same diffusion coefficient. The molecules $\mathbf{m} = [m_1, \dots, m_K]$, with $m_k \in \{a, b\}$, are released at time

$$X_k = (k - 1)T, \quad k = 1, \dots, K, \quad (1)$$

where T denotes the duration of the bit interval. Each molecule propagates independently from others in the environment based on a specific propagation mechanism (e.g., Brownian motion with positive drift). Similar to [22], we assume no collisions among the molecules. At the RX, a fully absorbing receiver detects the type of the molecule and removes it from the environment. The arrival time of a molecule released at time X_k is given by

$$Y_k = X_k + Z_k, \quad k = 1, \dots, K, \quad (2)$$

where Z_k denotes the random propagation time of a molecule until the first arrival, which is referred to as first hitting time. The received molecules $\hat{\mathbf{m}} = [\hat{m}_1, \dots, \hat{m}_K]$ are collected based on their arrival order; for example, two released molecules m_1 and m_2 that are received out of order, i.e. $Y_1 > Y_2$, results in $\hat{\mathbf{m}} = [m_2, m_1]$. Hence, we consider an asynchronous detection, which requires no synchronization between TX and RX [19]. Finally, the received molecules are mapped to the estimated bit sequence $\hat{\mathbf{b}} = [\hat{b}_1, \dots, \hat{b}_K]$.

A. Propagation Environment

We consider two mechanism by which the molecules propagate from the TX to the RX inside the fluid medium:

1) *Brownian motion without drift*: The first hitting time of diffusion-based channels without drift follows a Lévy distribution, with its probability density function (PDF) given by [29]

$$f_Z(z) = \sqrt{\frac{c}{2\pi z^3}} \exp\left(-\frac{c}{2z}\right), \quad z > 0, \quad (3)$$

and its cumulative distribution function (CDF) can be expressed as

$$F_Z(z) = \operatorname{erfc}\left(\sqrt{\frac{c}{2z}}\right), \quad z > 0, \quad (4)$$

with the scale parameter $c = d^2/(2D)$. The complementary error function $\operatorname{erfc}(x)$ is defined by $\operatorname{erfc}(x) = 2/\sqrt{\pi} \int_x^\infty e^{-t^2} dt$ and d denotes the distance between TX and RX. The diffusion coefficient of the released molecules is given by

$$D = \frac{k_B T_a}{6\pi\eta r}, \quad (5)$$

where $k_B = 1.38 \times 10^{-23}$ J/K corresponds to the Boltzmann constant and r denotes the radius of the molecules, respectively.

2) *Brownian motion with drift*: The first hitting time of diffusion-based channels with positive drift follows an inverse Gaussian distribution with its PDF given by [6]

$$f_Z(z) = \sqrt{\frac{\lambda}{2\pi z^3}} \exp\left(-\lambda \frac{(z - \mu)^2}{2\mu^2 z}\right), \quad z > 0, \quad (6)$$

and its CDF can be expressed as

$$F_Z(z) = \phi\left(\sqrt{\frac{\lambda}{z}}\left(\frac{z}{\mu} - 1\right)\right) + \exp\left(\frac{2\lambda}{\mu}\right) \phi\left(-\sqrt{\frac{\lambda}{z}}\left(\frac{z}{\mu} + 1\right)\right), \quad z > 0, \quad (7)$$

with mean $\mu = d/v$, the shape parameter $\lambda = d^2/(2D)$ and the CDF of the standard normal distribution $\phi(x) = 1/\sqrt{2\pi} \int_{-\infty}^x \exp(-t^2/2) dt$. The positive drift velocity from TX to RX is denoted by v . In case of no drift, the inverse Gaussian distribution turns into a Lévy distribution.

It is important to note that for diffusion-based channels without drift the first hitting time in a 3D environment with a spherical absorbing receiver can be modeled by a Lévy distribution with a scaling parameter [7]. However, for diffusion-based channels with drift, to the best of our knowledge, no closed-form expression for the first hitting time probability has been derived so far.

B. Background Noise

In diffusion-based MC it is very likely that the RX does not only capture molecules from the corresponding TX, but also from other sources (environment and/or other TXs). We refer to these unintended molecules as background noise. Similar to [16], we consider the following assumptions: (i) The number of unintended molecules in disjoint time intervals are independent; (ii) The number of captured unintended molecules does not favor any time instant; (iii) No two unintended molecules

are captured at exactly the same time. If these conditions are fulfilled then the number of unintended molecules captured by the RX can be modeled by a Poisson random process with rate λ . Thus, the inter-arrival time of the unintended molecules follows an exponential distribution with mean λ^{-1} .

III. BIT ERROR PROBABILITY ANALYSIS

Due to the random arrival time of the molecules, they may arrive out of order at the RX and, thus, transpositions occur [17]. In this section, we study the BEP caused by transposition errors. We present an analytical expression for the exact BEP and we derive computationally tractable approximations of the BEP by exploiting the different channel properties. Based on these results we analyze the BEP when background noise is not negligible.

A. Exact BEP with Negligible Background Noise

We divide the derivation of the exact BEP into two steps: First, we determine the probability that a particular permutation is received when a sequence of K molecules is released. Then, we derive the BEP caused by each permutation.

Let \mathcal{P}_K represent the set of all possible permutations on K released molecules.

$$\mathcal{P}_K = \{\pi_0, \pi_1, \dots, \pi_M\}, \quad (8)$$

with $M = K!$ and π_0 denotes permutation where the order of the released molecules does not change. Moreover, we denote $\pi_m(i)$ as the i th element of the permutation π_m (e.g., $\pi_0(i) = i \forall i$). The probability of receiving a particular permutation $\pi \in \mathcal{P}_K$, given that π_0 was released, can be described as

$$\Pr[\pi, T | \pi_0] = \Pr[Y_{\pi(1)} < Y_{\pi(2)} < \dots < Y_{\pi(K)}], \quad (9)$$

where $Y_{\pi(i)} = X_{\pi(i)} + Z_{\pi(i)}$, with $X_{\pi(i)} = \pi^*(i)T$ and $\pi^*(i) = (\pi(i) - 1)$. Hence, the arrival probability of a permutation $\pi \in \mathcal{P}_K$ can be written as

$$\Pr[\pi, T | \pi_0] = \Pr[\pi^*(1)T + Z_{\pi(1)} < \pi^*(2)T + Z_{\pi(2)}, \dots, \pi^*(K-1)T + Z_{\pi(K-1)} < \pi^*(K)T + Z_{\pi(K)}]. \quad (10)$$

Similar to [22], we assume that the molecules propagate independently from each other and, thus, (10) can be determined by

$$\begin{aligned} \Pr[\pi, T | \pi_0] &= \int_0^\infty f_Z(z_{\pi(K)}) \int_0^{z_{\pi(K)} + \Delta\pi(K)T} f_Z(z_{\pi(K-1)}) \dots \\ &\quad \int_0^{z_{\pi(3)} + \Delta\pi(3)T} \int_0^{z_{\pi(2)} + \Delta\pi(2)T} f_Z(z_{\pi(2)}) \int_0^{z_{\pi(1)}} f_Z(z_{\pi(1)}) dz_{\pi(1)} \dots dz_{\pi(K)}, \end{aligned} \quad (11)$$

with $\Delta\pi(i) = \pi(i) - \pi(i-1)$ and $f_Z(z)$ denotes the PDF of the Lévy and the inverse Gaussian distribution defined in (3) and (6), respectively.

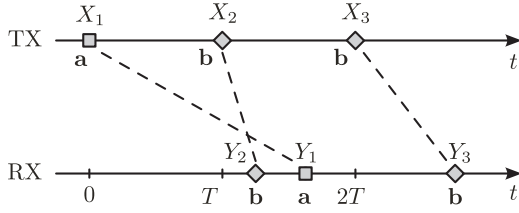


Fig. 1. Illustration of the transposition effect. Three molecules of type a , b and b are released at times X_1 , X_2 and X_3 and arrive at times Y_1 , Y_2 and Y_3 , with $Y_2 < Y_1 < Y_3$. Thus, the first and the second molecule are received out of order.

The BEP of a particular permutation can be derived by

$$\Pr[\hat{b}_k \neq b_k | \pi] = \frac{\text{disp}(\pi)}{2K}, \quad \pi \in \mathcal{P}_K. \quad (12)$$

The function $\text{disp}(\cdot)$ computes the number of displacements of a particular permutation $\pi \in \mathcal{P}_K$ and is defined by

$$\text{disp}(\pi) = \sum_{i=1}^K \left\lceil \frac{|\pi(i) - i|}{K} \right\rceil, \quad (13)$$

where the ceiling function $\lceil x \rceil$ denotes the mapping to the smallest following integer number.

Combining (9) and (12) gives the BEP due to transposition errors for the transmission of K bits

$$P_t^e = \Pr[\hat{b}_k \neq b_k] = \sum_{\pi \in \mathcal{P}_K} \Pr[b_k \neq \hat{b}_k | \pi] \Pr[\pi, T | \pi_0]. \quad (14)$$

However, the evaluation of (14) is only feasible for small block sizes K , since $|\mathcal{P}_K| = K!$. Hence, in the next section we present a computationally tractable approximation of the BEP.

Example 1. We consider the transmission of $K = 3$ information bits $\mathbf{b} = [b_1, b_2, b_3]$ with $b_k \in \{0, 1\}$. Thus, the molecules $\mathbf{m} = [m_1, m_2, m_3]$, with $m_k \in \{a, b\}$ are released at time $X_1 = 0$, $X_2 = T$, and $X_3 = 2T$. For $b_k = 0$ type- a molecules ($m_k = a$) and for $b_k = 1$ type- b molecules ($m_k = b$) are released, respectively. The released molecules propagate through the environment according to the mechanisms described in Section II-A. We assume that they arrive at the receive in the order $\hat{\mathbf{m}} = [m_2, m_1, m_3]$ as illustrated in Fig. 1. For this permutation $\pi(1) = 2$, $\pi(2) = 1$ and $\pi(3) = 3$ and $Y_2 < Y_1 < Y_3$ holds. According to (11), the probability to observe such a permutation at the receiver is given by

$$\begin{aligned} \Pr[\pi, T | \pi_0] &= \Pr[Y_2 < Y_1 < Y_3] \\ &= \int_0^\infty f_Z(z_3) \int_0^{z_3+2T} f_Z(z_1) \int_0^{z_1-T} f_Z(z_2) dz_2 dz_1 dz_3. \end{aligned}$$

As shown in Fig. 2, a permutation does not directly translate to bit errors. For the permutation $\hat{\mathbf{m}} = [m_2, m_1, m_3]$ no error occurs if the released molecules m_1 and m_2 are of the same type, i.e. $m_1 = m_2 = m$ with $m \in \{a, b\}$. According to (12), the BEP for the considered permutation π is given by

$$\Pr[\hat{b}_k \neq b_k | \pi] = \frac{1}{3},$$

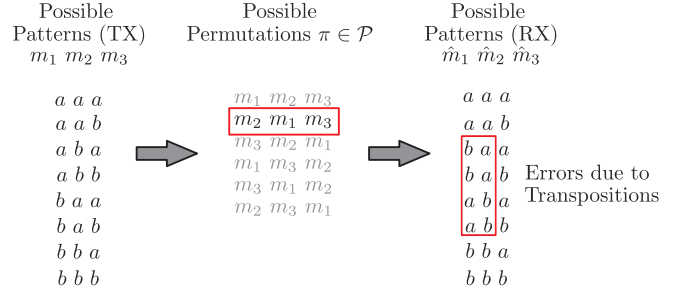


Fig. 2. Relation between permutation and bit error. If the first and the second molecule arrive out of order, i.e. $[m_1, m_2, m_3] \rightarrow [m_2, m_1, m_3]$, an error occurs only if the released molecules m_1 and m_2 are of different type.

with

$$\text{disp}(\pi) = \left\lceil \frac{|2-1|}{3} \right\rceil + \left\lceil \frac{|1-2|}{3} \right\rceil + \left\lceil \frac{|3-3|}{3} \right\rceil = 2.$$

B. Approximate BEP with Negligible Background Noise

We approximate the exact BEP given in (14) by exploiting the different properties of pure diffusion and drift channels. For drift channels, we assume that transpositions between neighboring bits are dominant and transpositions between bits that are more than one bit interval apart are negligible [16]. This assumption holds for $T > d/v$, which means that the average time of the molecules to arrive at the RX $\mu = d/v$ is smaller than the duration of one bit interval T . Unfortunately, this assumption does not hold for pure diffusion channels, since in this case the average arrival time of the molecules is infinity. For pure diffusion channels, we approximate the BEP based on the probability of out of order sequence delivery and the average BEP over these permutations.

1) *Diffusion-Based Channel Without Drift:* We define a lower bound for the arrival probability of the permutation π_0 , corresponding to in-sequence delivery of the released molecules. For this, we assume that all molecules arrive within the finite observation interval KT and, thus, the lower bound can be expressed as

$$\begin{aligned} \Pr[\pi_0, T | \pi_0] &\geq \Pr[Z_1 < KT, Z_2 < (K-1)T, \dots, Z_K < T] \\ &= \int_0^T f_Z(z_K) \cdots \int_0^{(K-1)T} f_Z(z_2) \int_0^{KT} f_Z(z_1) dz_1 \cdots dz_K \\ &= \prod_{j=1}^K F_Z(jT), \end{aligned} \quad (15)$$

where $F_Z(z)$ denotes the CDF of the Lévy distribution defined in (4). Hence, the arrival probability of all permutations except π_0 , i.e. $\mathcal{P}_K \setminus \{\pi_0\}$, is given by

$$\begin{aligned} \Pr[\mathcal{P}_K \setminus \{\pi_0\}, T | \pi_0] &= 1 - \Pr[\pi_0, T | \pi_0] \\ &\leq 1 - \prod_{j=1}^K F_Z(jT). \end{aligned} \quad (16)$$

Next, we derive the average BEP of the permutations in $\mathcal{P}_K \setminus \{\pi_0\}$. The following theorem allows to calculate the average value of $\text{disp}(\pi)$ in (13) over all permutations $\pi \in \mathcal{P}_K$.

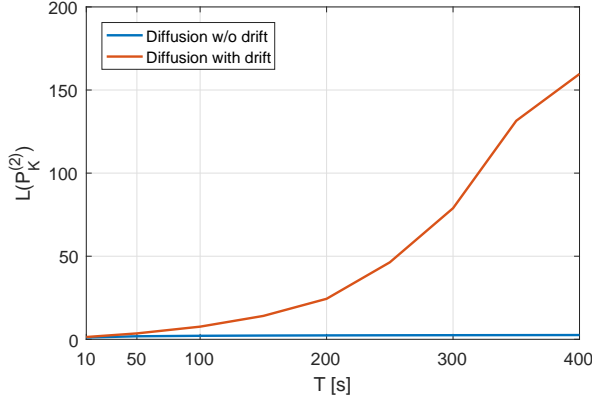


Fig. 3. Ratio between the arrival probability of permutations with single and multiple transpositions as defined in (22) for the simulation parameters in Tab. I with $K = 4$.

Theorem 1. Among all permutations of length $K \geq 1$ the average displacement is given by

$$\overline{\text{disp}}(\pi) = \frac{1}{K!} \sum_{\pi \in \mathcal{P}_K} \text{disp}(\pi) = K - 1, \quad (17)$$

with $\text{disp}(\pi) = \sum_{i=1}^K \lceil |\pi(i) - i|/K \rceil$ as defined in (13).

Proof. Let us assume to pick $i \in \{1, \dots, K\}$. Then the number of permutations $\pi \in \mathcal{P}_K$ that map i onto i' , i.e. $\pi(i) = i'$, is $(K-1)!$. Thus, we have

$$\sum_{\pi \in \mathcal{P}_K} \left\lceil \frac{|\pi(i) - i|}{K} \right\rceil = (K-1)(K-1)!. \quad (18)$$

Now, the average displacement can be obtained as follows

$$\begin{aligned} \overline{\text{disp}}(\pi) &= \frac{1}{K!} \sum_{\pi \in \mathcal{P}_K} \text{disp}(\pi) \\ &= \frac{1}{K!} \sum_{i=1}^K \sum_{\pi \in \mathcal{P}_K} \left\lceil \frac{|\pi(i) - i|}{K} \right\rceil \\ &= K - 1, \end{aligned} \quad (19)$$

with $\text{disp}(\pi) = \sum_{i=1}^K \lceil |\pi(i) - i|/K \rceil$ as defined in (13). \square

Replacing $\text{disp}(\pi)$ by $\overline{\text{disp}}(\pi)$ in (12) gives the average BEP of the permutations in $\mathcal{P}_K \setminus \{\pi_0\}$

$$\overline{\text{Pr}}[\hat{b}_k \neq b_k | \pi] = \frac{\overline{\text{disp}}(\pi)}{2K} = \frac{K-1}{2K}. \quad (20)$$

Now, we can define an upper bound for the BEP by using the arrival probability of the permutations in $\mathcal{P}_K \setminus \{\pi_0\}$ defined in (16) and their average BEP given in (20)

$$P_{\text{t}}^e = \text{Pr}[\hat{b}_k \neq b_k] \leq \frac{K-1}{2K} \left(1 - \prod_{j=1}^K F_Z(jT) \right). \quad (21)$$

In Sec. IV we show through numerical results that (21) provides a tight upper bound, and, thus, is an appropriate BEP approximation for diffusion-based channels without drift.

2) *Diffusion-Based Channel With Drift:* It can be shown that the tight upper bound derived in the previous section also holds for drift channels. However, in this section we derive another BEP approximation, exploiting the property that in drift channels transpositions between neighboring bits are dominant. Fig. 3 shows the ratio between the arrival probability of permutations with a single transposition between neighboring bits and the arrival probability of permutations with multiple permutations, which can be expressed as

$$L(\mathcal{P}_K^{(2)}) = \frac{\text{Pr}[\pi \in \mathcal{P}^{(2)}]}{\text{Pr}[\pi \in \mathcal{P}_K \setminus \{\pi_0 \cup \mathcal{P}^{(2)}\}]}. \quad (22)$$

The set $\mathcal{P}_K^{(2)} \subset \mathcal{P}_K$ includes only permutations with a single transposition between neighboring bits. We observe from Fig. 3 that by increasing the bit interval T the ratio $L(\mathcal{P}_K^{(2)})$ increases significantly for drift channels, but remains almost constant for pure diffusion channels. Thus, for drift channels it is very likely to receive a permutation with only a single permutation between neighboring bits instead of a permutation with multiple permutations. The probability of receiving a permutation $\pi \in \mathcal{P}_K^{(2)}$ can be expressed as³

$$\begin{aligned} \text{Pr}[\pi, T | \pi_0] &= \text{Pr}[Z_k > Z_{k+1} + T] \\ &= \text{Pr}[\Delta Z < -T], \quad k = 1, \dots, K-1. \end{aligned} \quad (23)$$

with the random variable $\Delta Z = Z_{k+1} - Z_k$, where Z_{k+1} and Z_k follow an inverse Gaussian distribution as defined in Sec. II-A. According to (12), the BEP of permutations $\pi \in \mathcal{P}^{(2)}$ is given by

$$\text{Pr}[b_k \neq \hat{b}_k | \pi] = \frac{1}{K}, \quad \pi \in \mathcal{P}^{(2)}, \quad (24)$$

with $\text{disp}(\pi) = 2$. Based on (23) and (24) the BEP for drift channels can be approximated as follows

$$\begin{aligned} P_{\text{t}}^e &= \text{Pr}[\hat{b}_k \neq b_k] = \sum_{\pi \in \mathcal{P}_K^{(2)}} \text{Pr}[b_k \neq \hat{b}_k | \pi] \text{Pr}[\pi, T | \pi_0] \\ &= \frac{K-1}{K} \text{Pr}[\Delta Z < -T] \\ &= \frac{K-1}{K} F_{\Delta Z}(-T), \end{aligned} \quad (25)$$

with $|\mathcal{P}_K^{(2)}| = K-1$. Moreover, $F_{\Delta Z}(\Delta z)$ denotes the CDF of the random variable ΔZ and probability $F_{\Delta Z}(-T) = 1 - F_{\Delta Z}(T)$ describes the tail probability of ΔZ . Unfortunately, no closed-form expressions exists for the distribution of ΔZ [30]. Thus, we apply a recently proposed moment matching approximation by a the normal

³It is important to note that the probability on the right hand side of (23) describes the arrival probability of all permutations with transposed bits k and $k+1$, irrespective of the position of the other bits in the permutation sequence. However, as stated above, the arrival probability is dominated by the permutation having only the bits k and $k+1$ swapped and the other bits are received in the correct order, i.e. $\pi \in \mathcal{P}_K^{(2)}$.

inverse Gaussian (NIG) distribution [30]. The PDF of the NIG distribution is given by

$$f_{\Delta Z}(\Delta z) = \frac{\alpha\delta}{\pi} \exp\left(\delta\sqrt{\alpha^2 - \beta^2} - \beta(\Delta z - \mu)\right) \times \frac{K_1\left(\alpha\sqrt{\delta^2 + (\Delta z - \mu)^2}\right)}{\sqrt{\delta^2 + (\Delta z - \mu)^2}}, \quad (26)$$

where $K_1(\cdot)$ denotes the modified Bessel function of the third kind with index 1 and the parameters are defined by [30]

$$\begin{aligned} \alpha &= \frac{1}{\sqrt{20}} \frac{v^2}{D}, & \beta &= 0, \\ \mu &= 0, & \delta &= \frac{2}{\sqrt{5}} \frac{d}{v}. \end{aligned} \quad (27)$$

C. BEP with non Negligible Background Noise

We approximate the BEP caused by transpositions and background noise by using the union bound

$$P^e \leq P_t^e + P_n^e, \quad (28)$$

where P_t^e denotes to the BEP due to transpositions (cf. (14), (21) and (25)). The BEP caused by background noise is denoted by P_n^e is given by [16]

$$P_n^e = \frac{1}{2} \left[\gamma(1, \xi T) - \frac{1}{\xi T} \gamma(2, \xi T) \right], \quad (29)$$

with $\xi = 2\lambda K$ and lower incomplete gamma function $\gamma(s, x)$. Exploiting some properties of the incomplete gamma function, i.e. $\gamma(1, \xi T) = 1 - \exp(-\xi T)$ and $\gamma(2, \xi T) = \gamma(1, \xi T) - \xi T \exp(-\xi T)$, the BEP expression due to background noise simplifies to

$$P_n^e = \frac{1}{2} \left[1 - \frac{1}{\xi T} - \frac{\exp(-\xi T)}{\xi T} \right]. \quad (30)$$

If the background noise is negligible the errors due to transpositions can be reduced by increasing the bit interval T (cf. Sec. IV). Unfortunately, if background noise is considered larger bit intervals increases the number of unintended molecules captured by the RX, which increases the BEP. Hence, there exists an optimal bit interval T_{opt} that minimizes the BEP, i.e.

$$T_{\text{opt}} = \underset{T}{\operatorname{argmin}} P^e(T). \quad (31)$$

In order to derive the optimal bit interval T_{opt} we solve the following equation

$$\frac{\partial P^e}{\partial T} = \frac{\partial P_t^e}{\partial T} + \frac{\partial P_n^e}{\partial T} = 0, \quad (32)$$

where we assumed a tight union bound, i.e. $P^e \approx P_t^e + P_n^e$. The first derivative of P_n^e can be calculated as follows

$$\frac{\partial P_n^e}{\partial T} = \frac{\exp(-\xi T) [-1 - \xi T + \exp(\xi T)]}{2\xi T^2}. \quad (33)$$

For the first derivative of P_t^e we use the approximate BEP expression for pure diffusion and drift channels given in (21) and (25), respectively. For pure diffusion channels, the first

TABLE I
SIMULATION PARAMETERS

Parameter	Value
Velocity v	$\{0, 1\} \mu\text{m/s}$
Block size K	20
Distance d	10 μm
Diff. Coeff D	28.369 $\mu\text{m}^2/\text{s}$
Noise Generation Rate λ	$1 \times 10^{-6} \text{s}^{-1}$

derivative can be calculated by applying the generalized product rule, which results in

$$\frac{\partial P_t^e}{\partial T} = -\frac{K-1}{2K} \prod_{j=1}^K F_Z(jT) \sum_{j=1}^K \frac{j f_Z(jT)}{F_Z(jT)}, \quad (34)$$

where $f_Z(z)$ and $F_Z(z)$ denote the PDF and CDF of the Lévy distribution as defined in (3) and (4). For drift channels, the first derivative is given by

$$\frac{\partial P_t^e}{\partial T} = -\frac{K-1}{K} f_{\Delta Z}(-T). \quad (35)$$

where $f_{\Delta Z}(\Delta z)$ corresponds to the PDF of the NIG distribution given in (26). Finally, we obtain the optimal bit interval T_{opt} by numerically solving

$$\left. \frac{\partial P^e(T)}{\partial T} \right|_{T=T_{\text{opt}}} = 0, \quad (36)$$

using (33) – (35).

IV. SIMULATION RESULTS

In this section, we investigate the error and goodput performance under different operating conditions. The goodput G represents the number of successfully received bits per block and can be expressed as

$$G = (1 - P^e)K, \quad (37)$$

where P^e denotes the BEP caused by transpositions and background noise as defined in (28). The probability for a successful bit reception is given by $(1 - P^e)$ and K is the block size. We also show the accuracy of the BEP approximations derived in Secs. III-B and III-C. In the simulations, we considered a one-shot communication [31], which means that the TX sends a block of K information bits to the RX and then remains silent for a long period⁴. In particular, we assumed that all released molecules of a block eventually arrive at the RX (infinite lifetime) and the TX remains silent until all molecules are captured by the RX. However, we consider a finite observation duration at the RX i.e. the RX collects molecules up to time KT . Each data point in the simulations was obtained by generating $N = 10^6$ uniformly distributed bits which are split up into K blocks that are sent independently of each other to the RX (one-shot communication). Thus, no transpositions across the blocks occur. If not otherwise stated, we used the simulation parameters in Tab. I. The diffusion coefficient $D = 28.369 \mu\text{m}^2/\text{s}$ is obtained by (5), substituting $T_a = 310 \text{K}$

⁴For example, a nano-sensor that infrequently sends data to a RX.

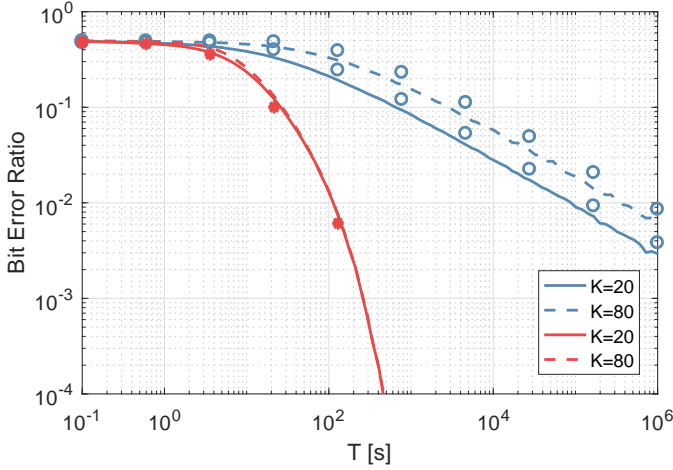


Fig. 4. BER versus bit interval T for different block sizes K without background noise. Blue and red curves: Simulated BER for pure diffusion and drift channels; Circle and star marker: Theoretical BEP approximation for pure diffusion and drift channels as discussed in Sec. III-B.

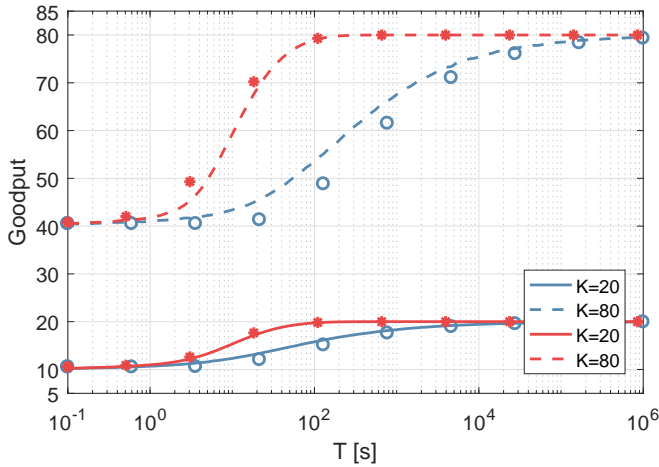


Fig. 5. Goodput versus bit interval T for different block sizes K without background noise. Blue and red curves: Simulated goodput for pure diffusion and drift channels; Circle and star marker: Theoretical goodput approximation for pure diffusion and drift channels as discussed in Sec. IV.

(body temperature), venous blood viscosity $\eta = 0.004 \text{ Pa} \cdot \text{s}$ and molecule radius $r = 2 \text{ nm}$ [16]. We assumed that the radius of the molecules is negligible compared to the distance between TX and RX, i.e. $r \ll d$. In all figures⁵, the blue curves indicate the BER results for pure diffusion channels ($v = 0 \mu\text{m/s}$) and the red curves show the BER results for drift channels ($v = 1 \mu\text{m/s}$). Moreover, the circle and star markers indicate the theoretical BEP approximation for pure diffusion and drift channels derived in Secs. III-B and III-C.

A. Performance with Negligible Background Noise

Figs. 4 – 7 show the error and goodput performance for different blocks sizes K , distances d and diffusion coefficients D without background noise, i.e. $\lambda = 0 \text{ s}^{-1}$. We observe that the BER decreases as the bit interval T increases, since this lowers the probability of transpositions. The BER for drift channels

⁵For the interpretation of the references to the color in all figures, the reader is referred to the web version of this article.

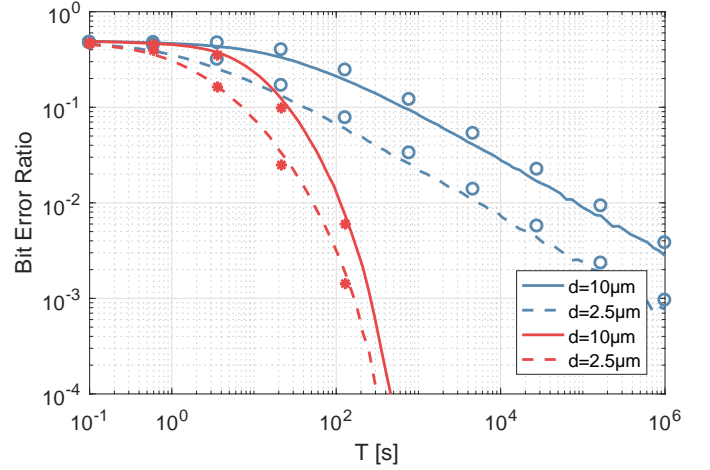


Fig. 6. BER versus bit interval T for different distances d without background noise. Blue and red curves: Simulated BER for pure diffusion and drift channels; Circle/star marker: Theoretical BEP approximation for pure diffusion and drift channels as discussed in Sec. III-B.

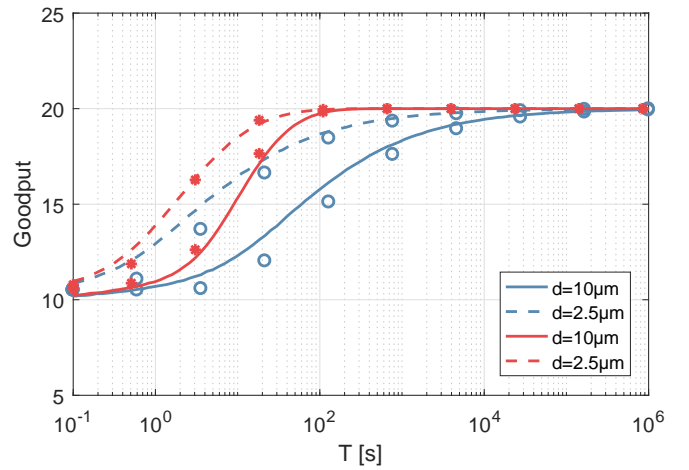


Fig. 7. Goodput versus bit interval T for different distances d without background noise. Blue and red curves: Simulated goodput for pure diffusion and drift channels; Circle and star marker: Theoretical goodput approximation for pure diffusion and drift channels as discussed in Sec. IV.

decreases significantly faster than for pure diffusion channels. This is because in drift channels single transpositions between neighboring bits are dominant for large bit intervals T (cf. Fig. 3). Moreover, for drift channels the goodput reaches its maximum K , i.e. all K released bits are received successfully, already for smaller bit intervals compared to pure diffusion channels. Although, the BER decreases and the goodput increases as the bit interval increases, also the transmission time increases with an increasing bit interval. Thus, the bit interval allows a tradeoff between reliability and transmission time. In Figs. 4, 6 and 8 we also compare the theoretical BEP approximations in (21) and (25) with the simulated BER. We show that for drift channels they match very well and we observe that the upper bound derived for pure diffusion channels is tight. Similar observations can be made for the goodput performance shown in Figs. 5, 7 and 9, where the theoretical goodput approximation is obtained using (37), with $P^e \approx P_t^e$ and using the BEP approximations in (21) and (25)

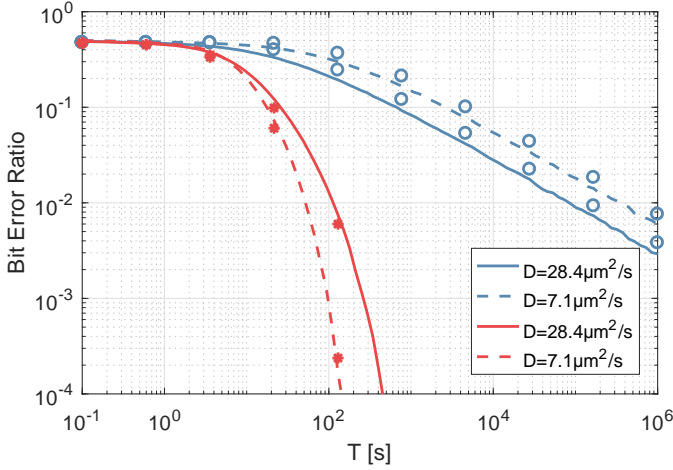


Fig. 8. BER versus bit interval T for different diffusion coefficients D without background noise. Blue and red curves: Simulated BER for pure diffusion and drift channels; Circle and star marker: Theoretical BEP approximation for pure diffusion and drift channels as discussed in Sec. III-B.

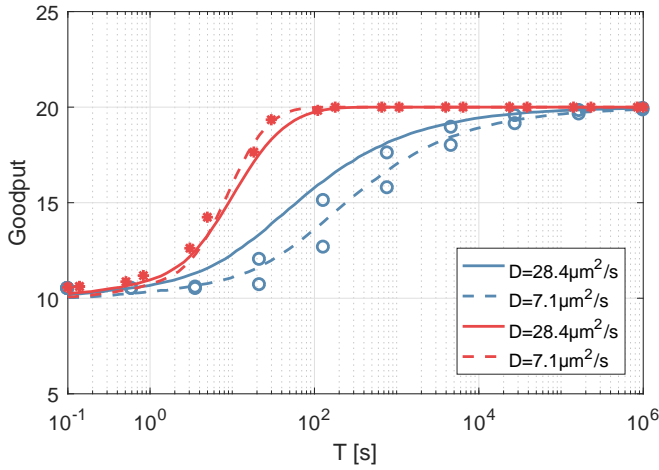


Fig. 9. Goodput versus bit interval T for different diffusion coefficients D without background noise. Blue and red curves: Simulated goodput for pure diffusion and drift channels; Circle and star marker: Theoretical goodput approximation for pure diffusion and drift channels as discussed in Sec. IV.

for P_t^c .

Figs. 4 and 5 show the BER and goodput performance versus the bit interval T for $K \in \{20, 80\}$, respectively. We observe from Fig. 4 that increasing the block size results in a slight loss in the BER performance for drift channels, but a significant performance degradation for pure diffusion channels. This is because in drift channels the error performance is dominated by single transpositions irrespective of the block size and for pure diffusion channels more transpositions occur as the block size increases. A similar observation can be made for the goodput in Fig. 5. For drift channels the bit interval at which the goodput reaches its maximum K is almost independent of the block size, but for pure diffusion channels it increases as the block size increases.

Figs. 6 and 7 show the BER and goodput performance versus the bit interval T for $d \in \{2.5, 10\} \mu\text{m}$. We observe that the BER decreases as the distance decreases. Moreover, for small distances the goodput is higher for a certain bit interval and

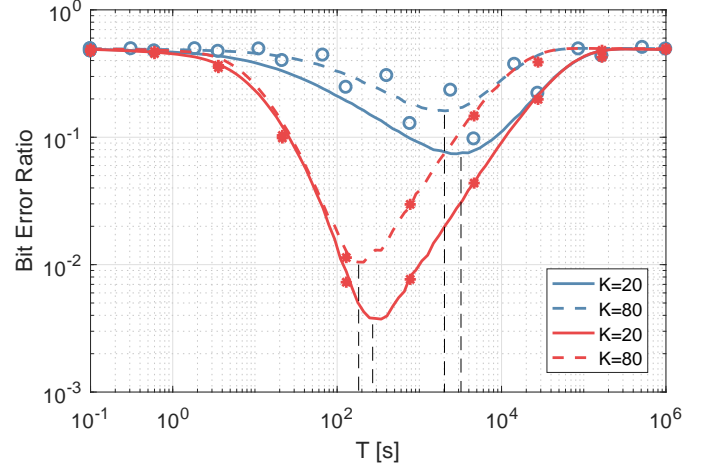


Fig. 10. BER versus bit interval T for different block sizes K with noise generation rate $\lambda = 1 \times 10^{-6} \text{ s}^{-1}$. Blue and red curves: Simulated BER for pure diffusion and drift channels; Circle and star marker: Theoretical BEP approximation for pure diffusion and drift channels as discussed in Secs. III-B and III-C. The optimal bit interval T_{opt} derived from (36) for pure diffusion and drift channels is given by $\{183, 271\} \text{ s}$ and $\{2022, 3212\} \text{ s}$, respectively.

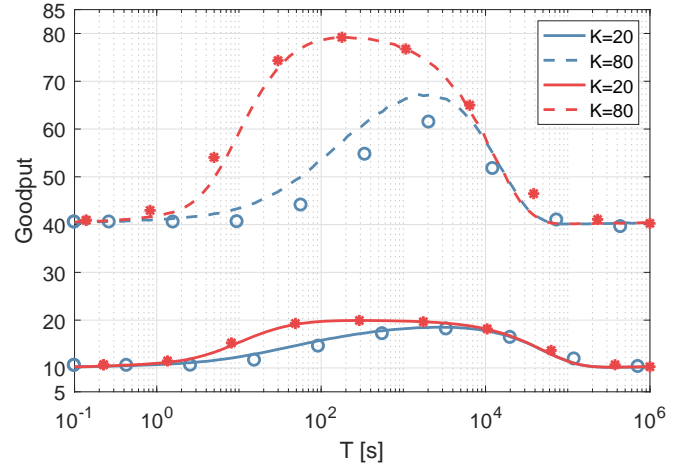


Fig. 11. Goodput versus bit interval T for different block sizes K with noise generation rate $\lambda = 1 \times 10^{-6} \text{ s}^{-1}$. Blue and red curves: Simulated goodput for pure diffusion and drift channels; Circle and star marker: Theoretical goodput approximation for pure diffusion and drift channels as discussed in Sec. IV.

the maximum K is reached faster.

Figs. 8 and 9 show the BER and goodput performance versus the bit interval T and versus the goodput for $D \in \{7.1, 28.4\} \mu\text{m}^2/\text{s}$. The diffusion coefficient $D = 7.1 \mu\text{m}^2/\text{s}$ is obtained by increasing the molecule radius from $r = 2 \text{ nm}$ to $r = 8 \text{ nm}$. Interestingly, we observe from Fig. 8 that for drift channels the BER decreases if the radius of the released molecules is increased (lower diffusion coefficient) [32]. This is because larger molecules experience more support due to drift compared to small molecules. However, for pure diffusion channels the performance decreases when the molecule radius is increased. Hence, for drift channels the goodput is improved by releasing larger molecules, but for pure diffusion channels this results in a degradation of the goodput.

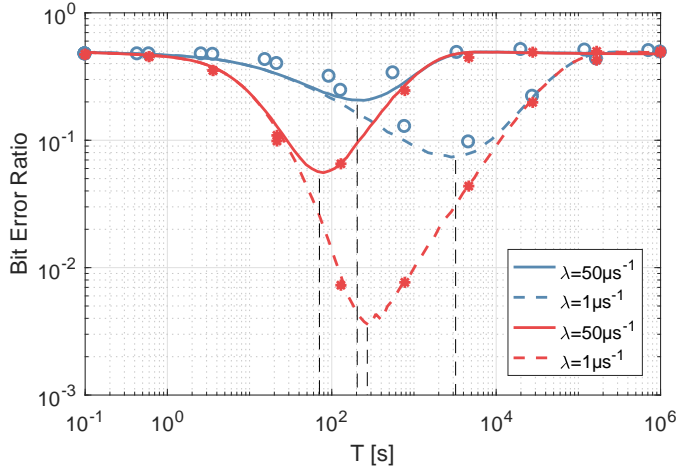


Fig. 12. BER versus bit interval T for different noise generation rates λ . Blue and red curves: Simulated BER for pure diffusion and drift channels; Circle and star marker: Theoretical BEP approximation for pure diffusion and drift channels as defined in Secs. III-B and III-C. The optimal bit interval T_{opt} derived from (36) for pure diffusion and drift channels is given by $\{71, 271\}$ s and $\{204, 3212\}$ s, respectively.

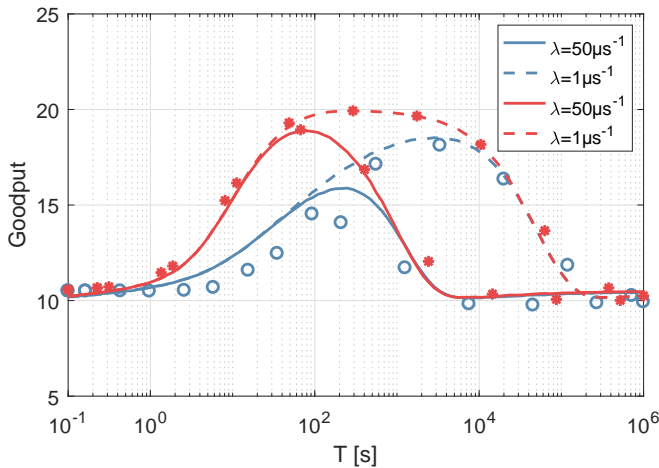


Fig. 13. Goodput versus bit interval T for different noise generation rates λ . Blue and red curves: Simulated BER for pure diffusion and drift channels; Circle and star marker: Theoretical BEP approximation for pure diffusion and drift channels as defined in Sec. IV.

B. Performance without Negligible Background Noise

Figs. 10 – 13 show the error and goodput performance when background noise is considered. Moreover, we compare the theoretical BEP approximation derived in Secs. III-B and III-C and the theoretical goodput performance defined in (37) with the simulation results. We observe a good match between the theoretical and simulation results. As shown in Secs. IV-A, the BER can be improved by increasing the bit interval. However, if background noise is not negligible an optimal bit interval T_{opt} exists, which minimizes the BER (cf. Sec. III-C). The optimal bit interval derived from (36) is depicted in Figs. 10 and 12, showing a good match between the analytical and the numerical results.

Figs. 10 and 11 show the BER and goodput performance versus the bit interval T for $K \in \{20, 80\}$, considering

background noise with rate $\lambda = 1 \times 10^{-6} \text{ s}^{-1}$. We observe that up to the optimal bit interval the BER decreases with the same slope as in the case without background noise (cf. Fig. 4), i.e. errors due to transpositions are dominant. After the optimal bit interval the BER increases again, i.e. errors due to background noise become dominant. Similarly, the goodput increases until the optimal bit interval and then decreases again. It is important to note that in contrast to the scenario without background noise the goodput does not necessarily achieve its maximum K . Figs. 12 and 13 show the BER and goodput performance versus the bit interval T for $\lambda \in \{50, 1\} \mu\text{s}^{-1}$. We observe that if the noise generation rate λ is increased the optimal bit interval decreases, i.e. the minimum achievable BER is reduced. Similarly, the maximum achievable goodput becomes lower as the noise generation rate increases.

V. CONCLUSIONS

We studied the impact of transposition errors on the performance of diffusion-based MC with and without drift. We used type-based information encoding releasing a single molecule per information bit and the detection algorithm exploited the arrival order of the molecules. We presented an analytical expression for the exact BEP and derived computationally tractable approximation of the BEP for pure diffusion and drift channels. Then, we considered background noise and derived an approximation of the BEP and the optimal bit interval minimizing the BEP. We verified the theoretical results through simulation results. Moreover, numerical results revealed a huge performance gain for drift channels compared to pure diffusion channels in terms of error rate and goodput. Thus, pure diffusion-based MC is only appropriate for short block sizes and if the transmission time is not crucial. Extending the presented results for information encoding using more than two types of molecules would be an interesting future work. This would significantly reduce the error rate and the transmission time.

REFERENCES

- [1] T. Nakano, A. Eckford, and T. Haraguchi, *Molecular Communication*. Cambridge University Press, 2013.
- [2] N. Farsad, H. B. Yilmaz, A. Eckford, C. B. Chae, and W. Guo, “A comprehensive survey of recent advancements in molecular communication,” *IEEE Commun. Surveys Tuts.*, vol. 18, no. 3, pp. 1887–1919, thirdquarter 2016.
- [3] T. D. Wyatt, *Pheromones and Animal Behaviour: Communication by Smell and Taste*. Cambridge University Press, 2003.
- [4] C. Rose and I. Mian, “A fundamental framework for molecular communication channels: Timing and payload,” in *Proc. IEEE Int. Conf. Commun.*, June 2015, pp. 1043–1048.
- [5] M. Pierobon and I. F. Akyildiz, “Diffusion-based noise analysis for molecular communication in nanonetworks,” *IEEE Trans. Signal Process.*, vol. 59, no. 6, pp. 2532–2547, June 2011.
- [6] K. V. Srinivas, A. W. Eckford, and R. S. Adve, “Molecular communication in fluid media: The additive inverse Gaussian noise channel,” *IEEE Trans. Inf. Theory*, vol. 58, no. 7, pp. 4678–4692, July 2012.
- [7] H. B. Yilmaz, A. C. Heren, T. Tugcu, and C. B. Chae, “Three-dimensional channel characteristics for molecular communications with an absorbing receiver,” *IEEE Commun. Lett.*, vol. 18, no. 6, pp. 929–932, June 2014.
- [8] B. H. Koo, C. Lee, H. B. Yilmaz, N. Farsad, A. Eckford, and C. B. Chae, “Molecular MIMO: From theory to prototype,” *IEEE J. Sel. Areas Commun.*, vol. 34, no. 3, pp. 600–614, Mar. 2016.

- [9] N. Farsad, D. Pan, and A. J. Goldsmith, "A novel experimental platform for in-vessel multi-chemical molecular communications," in *Proc. IEEE Global Telecommunications Conference*, Dec. 2017, pp. 1 – 6.
- [10] A. Llopis-Lorente, P. Diez, A. Sanchez, M. D. Marcos, F. Sancenon, P. Martinez-Ruiz, R. Villalonga, and R. Martnez-Manez, "Interactive models of communication at the nanoscale using nanoparticles that talk to one another," *Nature Commun.*, pp. 1–7, 2017.
- [11] Y. Chahibi, "Molecular communication for drug delivery systems: A survey," *Nano Commun. Netw.*, vol. 11, pp. 90 – 102, 2017.
- [12] U. A. K. Okonkwo, R. Malekian, B. T. Maharaj, and A. V. Vasilakos, "Molecular communication and nanonetwork for targeted drug delivery: A survey," *IEEE Commun. Surveys Tuts.*, vol. PP, no. 99, pp. 1–1, 2017.
- [13] L. Felicetti, M. Femminella, G. Reali, and P. Lio, "Applications of molecular communications to medicine: A survey," *Nano Commun. Netw.*, vol. 7, pp. 27 – 45, 2016.
- [14] M. U. Mahfuz, D. Makrakis, and H. T. Mouftah, "Concentration-encoded subdiffusive molecular communication: Theory, channel characteristics, and optimum signal detection," *IEEE Trans. Nanobiosci.*, vol. 15, no. 6, pp. 533–548, Sept 2016.
- [15] H. Arjmandi, M. Movahednasab, A. Gohari, M. Mirmohseni, M. Nasiri-Kenari, and F. Fekri, "ISI-avoiding modulation for diffusion-based molecular communication," *IEEE Trans. Mol., Biol. Multi-Scale Commun.*, vol. 3, no. 1, pp. 48–59, March 2017.
- [16] Y. K. Lin, W. A. Lin, C. H. Lee, and P. C. Yeh, "Asynchronous threshold-based detection for quantity-type-modulated molecular communication systems," *IEEE Trans. Mol., Biol. Multi-Scale Commun.*, vol. 1, no. 1, pp. 37–49, March 2015.
- [17] P. C. Yeh, K. C. Chen, Y. C. Lee, L. S. Meng, P. J. Shih, P. Y. Ko, W. A. Lin, and C. H. Lee, "A new frontier of wireless communication theory: Diffusion-based molecular communications," *IEEE Wireless Commun.*, vol. 19, no. 5, pp. 28–35, Oct. 2012.
- [18] Y. Murin, N. Farsad, M. Chowdhury, and A. Goldsmith, "Time-slotted transmission over molecular timing channels," *Nano Commun. Netw.*, vol. 12, pp. 12 – 24, 2017.
- [19] Y.-P. Hsieh, Y.-C. Lee, P.-J. Shih, P.-C. Yeh, and K.-C. Chen, "On the asynchronous information embedding for event-driven systems in molecular communications," *Nano Comm. Netw.*, vol. 4, pp. 2–13, 2013.
- [20] W. Haselmayr, S. M. H. Aejaz, A. T. Asyhari, A. Springer, and W. Guo, "Transposition errors in diffusion-based mobile molecular communication," *IEEE Commun. Lett.*, vol. 21, no. 9, pp. 1973–1976, Sept 2017.
- [21] A. Ahmadzadeh, V. Jamali, and R. Schober, "Statistical analysis of time-variant channels in diffusive mobile molecular communications," accepted to IEEE Global Commun. Conf., Dec. 2017.
- [22] T. Nakano and M. J. Moore, "In-sequence molecule delivery over an aqueous medium," *Nano Commun. Netw.*, vol. 1, pp. 181–188, 2010.
- [23] P. Manocha, G. Chandwani, and S. Das, "Dielectrophoretic relay assisted molecular communication for in-sequence molecule delivery," *IEEE Trans. Nanobiosci.*, vol. 15, no. 7, pp. 781–791, Oct 2016.
- [24] P.-Y. Ko, Y.-C. Lee, P. C. Yeh, C. han Lee, and K. C. Chen, "A new paradigm for channel coding in diffusion-based molecular communications: Molecular coding distance function," in *Proc. IEEE Global Commun. Conf.*, Dec 2012, pp. 3748–3753.
- [25] P. J. Shih, C. H. Lee, P. C. Yeh, and K. C. Chen, "Channel codes for reliability enhancement in molecular communication," *IEEE J. Sel. Areas Commun.*, vol. 31, no. 12, pp. 857–867, Dec 2013.
- [26] S. Qiu, T. Asyhari, and W. Guo, "Mobile molecular communications: Positional distance codes," in *Proc. IEEE Workshop Signal Process. Advances Wireless Commun.*, July 2016, pp. 1–6.
- [27] P. R. C. Gascoyne, "Cell dielectric properties as diagnostic markers for tumor cell isolation," in *Tumor Markers: Physiology, Pathobiology, Technology, and Clinical Applications*, 2002.
- [28] L. Kang, "Microfluidics for drug discovery and development: From target selection to product lifecycle management," *Drug Discovery Today*, vol. 13, no. 1, pp. 1 – 13, 2008.
- [29] N. Farsad, W. Guo, C. B. Chae, and A. Eckford, "Stable distributions as noise models for molecular communication," in *Proc. IEEE Global Commun. Conf.*, Dec 2015, pp. 1–6.
- [30] W. Haselmayr, D. Efrosinin, and W. Guo, "Normal inverse Gaussian approximation for molecular communications," submitted to IEEE Trans. Mol., Biol. Multi-Scale Commun., 2018.
- [31] Y. Murin, M. Chowdhury, N. Farsad, and A. Goldsmith, "Diversity gain of one-shot communication over molecular timing channels," in *Proc. IEEE Global Commun. Conf.*, Dec 2017, pp. 1–6.
- [32] T. Furubayashi, T. Nakano, A. Eckford, Y. Okaie, and T. Yomo, "Packet fragmentation and reassembly in molecular communication," *IEEE Trans. Nanobiosci.*, vol. 15, no. 3, pp. 284–288, April 2016.